Condition monitoring of squirrel cage induction machine using neuro controller

Article *in* Journal of Electrical Engineering · March 2016

3 authors, including:

Premkumar Manoharan
Dayananda Sagar College of Engineering
124 PUBLICATIONS   2,115 CITATIONS

SEE PROFILE

Some of the authors of this publication are also working on these related projects:

Project   Induction motor condition monitoring View project

Project   Regenerative braking in electric vehicle View project

CONDITION MONITORING OF SQUIRREL CAGE INDUCTION MACHINE USING NEURO CONTROLLER

[1]M.Premkumar, [2]A.Mohamed Ibrahim, [3]Dr.T.R.Sumithira

[1,2]Assistant professor in Department of Electrical & Electronics Engineering, KPR Institute of Engg. & Tech., Coimbatore

[3]Professor in Department of Electrical & Electronics Engineering, KSR College of Engineering, Tiruchengode

[1]mprem.me@gmail.com, [2]mohamedgct06@gmail.com, [3]sumithira.trs@gmail.com

ABSTRACT – The proposed work aims at the implementation of Motor Current Signature Analysis (MCSA) for detecting the bearing fault in squirrel cage induction motor. This proposed scheme monitors the stator current spectrum to detect the bearing faults and to extract fault signature by using Fast Fourier Transform (FFT) analyzer. For fault diagnosis, Neural Network (NN) is used. The fault detection scheme is implemented in real time. Since this scheme detect the faults at their earlier stage, the maintenance can be carried out in organized manner, which reduces the down time and repairing cost. This approach is validated in a 1 HP 415V 50HZ 960-rpm three phase induction motor.

Keyword – MCSA, Bearing Fault, FFT Analyzer, Neural Network.
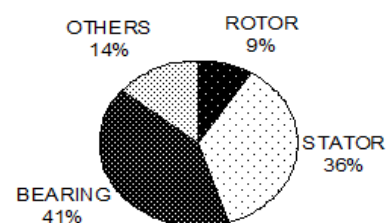
I. INTRODUCTION

The simple, robust design and construction of AC induction motor have encouraged their successful in industry for many years. However, these motors are required to operate in highly corrosive and dusty environments. These factors coupled with the natural aging process of any motor make the motor subject to faults. These faults if undetected, contribute to the degradation and eventual failure of the motors. As it is not economical to introduce redundant backup motors, condition monitoring for induction motor is important for safe operation. In order to keep the motor condition, techniques such as fault monitoring, detection, classification and diagnosis have become increasingly essential. Earlier detection of the fault reduces repair cost and motor outage time thereby improving safety [1].

In general, condition monitoring schemes have concentrated on specific failures modes in one of three phase induction motor components: the stator, the rotor, or bearings. Even though thermal and vibration monitoring have been utilized for decades, most of the recent research has been directed toward electrical monitoring of the motor with emphasis on inspecting the stator current of the motor.

1.1 Bearing Faults in Induction Motors

Bearings play an important role in the reliability and performance of all motor systems. In addition, most faults arising in motors are often linked to bearing faults. The result of many studies show that bearing problems account for over 40% of all machine failures [3]. The several faults and its percentage are shown in the Figure 1.1.

Figure 1.1 Faults in Induction Motor

1.2 Necessity of a Monitoring System

Machine condition monitoring is gaining importance in industry because of the need to increase reliability and to decrease the possibility of production loss due to machine breakdown. By comparing the signals of a machine running in normal and faulty conditions, detection of faults like mass unbalance, rotor rub, shaft misalignment, gear failures, and bearing defects is possible. These signals can also be used to detect the incipient failures of the machine components, through the online monitoring system, reducing the possibility of catastrophic damage and the downtime. Although often the visual inspection of the frequency domain features of the measured signals is adequate to identify the faults, there is a need for a reliable, fast, and automated procedure of diagnostics. Artificial intelligence techniques like Neural Fuzzy techniques can be implemented in the system for automated detection and diagnosis of machine conditions [5].

1.3 Bearing Structural Defects

Rolling element bearings generally consist of two rings, an inner and an outer race, between which a set of balls or rollers rotate in raceways. Under normal operating conditions of balanced load and good alignment, fatigue failure begins with small fissures, located between the surface of the raceway and the rolling elements, which gradually propagate to the surface generating detectable vibrations and increasing noise levels. Continued stress causes fragments of the material to break loose, producing a localized fatigue phenomenon known as flaking or spalling. Once started, the affected area expands rapidly contaminating the lubricant and causing localized overloading over the entire circumference of the raceway. Eventually, the failure results in rough running of the bearing. While this is the normal mode of failure in rolling element bearings, there are many other conditions which reduce the time to bearing failure. These external sources include contamination, corrosion, improper lubrication, and improper installation [8], [9].

Contamination and corrosion frequently accelerate bearing failure because of the harsh environments present in most industrial settings. Dirt and other foreign matter that is commonly present often contaminate the bearing lubrication.
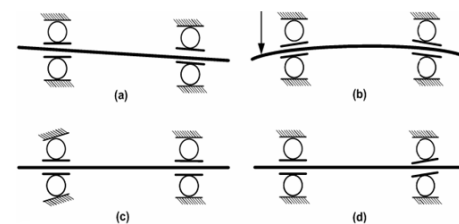
Figure1.2 Misalignment of the Bearing
(a) Misalignment (out-of-line),
(b) Shaft deflection,
(c) Crooked or tilted outer race,
(d) Crooked or tilted inner race.

Bearing corrosion is produced by the presence of water, acids, deteriorated lubrication and even perspiration from careless handling during installations. Improper lubrication includes both under- and over-lubrication. In either case, the rolling elements are not allowed to rotate on the designed oil film causing increased levels of heating. The excessive heating causes the grease to break down, which reduces its ability to lubricate the bearing elements and accelerates the failure process. Installation problems are often caused by

improperly forcing the bearing onto the shaft or in the housing. This produces physical damage in the form of brinelling or false brinelling of the raceways which leads to premature failure. Misalignment of the bearing, which occurs in the four ways depicted in Figure 1.2, is also a common result of defective bearing installation. The most common of these is caused by tilted races. Brinelling is the formation of indentations in the raceways as a result of deformation caused by static overloading.

II. BEARING FAULT DETECTION

2.1. Problem Definition

The relationship of the bearing vibration to the stator current spectrum can be determined by remembering that any air-gap eccentricity produces anomalies in the air-gap flux density. In the case of a dynamic eccentricity that varies with rotor position, the oscillation in the air-gap length causes variations in the air-gap flux density. This variation affects the inductance of the machine producing stator current harmonics. Since ball bearings support the rotor, any bearing defect produces a radial motion between the rotor and the stator of the machine. The cause of air-gap eccentricity, these variations generate harmonic stator currents at predictable frequencies, related to the vibration and electrical supply frequencies by

$$f_{bng} = |f_e \pm m \cdot f_v| \qquad \text{...... (2.1)}$$

Where $m = 1, 2, 3, . ,$ *etc* and f_v is one of the characteristic vibration frequencies.

The characteristic frequency of bearing failure (bearing pass frequency) is the inverse number of the time between occurrences of bearing impulses. This frequency can be calculated by the aid of known bearing geometry and rotational speed. The dimensions of a bearing are given in the Figure 2.1. An outer race defect causes impulse when ball or roller passes the defected area of race. The theoretical frequency is thus

$$f_o = \frac{N}{2} \cdot f_r \cdot \left(1 - \frac{d}{D} \cdot \cos\alpha\right) \qquad \text{...... (2.2)}$$

where N is the number of balls or rollers, fr is the rotational speed of rotor, d is the diameter of thzall, D is the pitch diameter, α is a contact angle of rolling element. The ball pass frequency of defect on inner race is

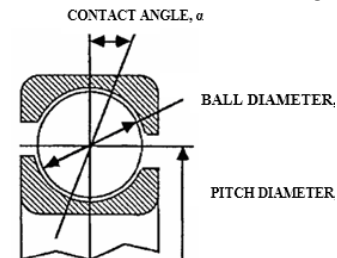$$f_i = \frac{N}{2} \cdot f_r \cdot \left(1 + \frac{d}{D} \cdot \cos\alpha\right) \qquad \text{...... (2.3)}$$

The ball spin frequency is,

$$f_b = \frac{D}{2d} \cdot f_r \cdot \left(1 - \left(\frac{d}{D}\right)^2 \cdot \cos^2\alpha\right) \qquad \text{...... (2.4)}$$

and the cage fault frequency is,

$$f_c = \frac{1}{2} \cdot f_r \cdot \left(1 + \frac{d}{D} \cdot \cos\alpha\right) \qquad \text{...... (2.5)}$$

The frequencies of equations (2.3), (2.4), and (2.5) are valid for ideal bearing.

Figure 2.1 Dimensions of a Ball Bearing

In practice, the roller elements not only rotate on races but also slide. This can be taken into account by multiplying the theoretical frequencies with a sliding factor 'α' that usually takes value between 0.8 and 1.0. Very often in literature and in practice the above equations are replaced by

approximate equations. For example, for outer race defect

$$f_o = 0.4 \cdot N \cdot f_r \quad \dots\dots (2.6)$$

and for inner race defect

$$f_i = 0.6 \cdot N \cdot f_r \quad \dots\dots (2.7)$$

The simplified equations are used for two reasons, the geometry of the bearing is often not known and the actual condition monitoring device can calculate easily the frequencies of Equations (2.6) and (2.7) for couple of possible numbers of rolling elements [9].

2.2 Fault Detection Scheme

The purpose of the monitoring system is to measure the induction motor stator current and to analyze these data determining the vibration frequencies on the bearing. The stator current is sensed in any one of the three phases of the induction motor and its equivalent voltage signal is given to the sound cord of a PC. The analog signal Captured through the sound cord and it converts the sampled signal whose frequency is 11.025 kHz, to the frequency domain using Fast Fourier transform (FFT) algorithm. The current spectrum is generated by the FFT algorithm with 131072 points and includes only the magnitude information in decibels for each frequency component. The magnitude corresponding to the fault frequencies are extracted and it is given to the fault detection algorithm which is implemented using neural network. Condition of the bearing will be given as a result of that neural network module. Using the FFT analyzer the spectral values obtained and the required side band at ($ f^{*}_{bng} = \left| f_s \pm m f_{i,0} \right| $) value is measured. The

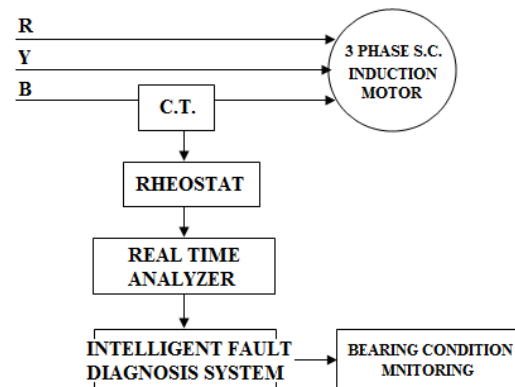single phase stator current monitoring scheme is shown in the Figure 2.2.

Figure 2.2 Single-Phase Stator Current Monitoring Scheme

2.3 Experimental Setup for Data Acquisition

To illustrate the fault detection scheme a 1 HP, six-pole induction motor is used .The rating of motor is given in Table 2.1. Figure 2.3 shows the experimental setup and for data acquisition. The bearings of the induction motor are single row, deep groove ball bearings, type 6204Z (Shaft end) and 6203Z (Fan end). Each bearing has 8 balls. Experiments were conducted on 5 bearings: two of these are undamaged (healthy), while three bearings were drilled through the outer race and inner race with holes of diameters 2mm and 3mm as illustrated in Figure 2.4.

Table 2.1 Rated parameters of the machine under test

Type	Three Phase Induction Motor
Power	1 HP
Voltage	415 V
Frequency	50 Hz
Current	1.8 A
Speed	960 rpm
Pole	6
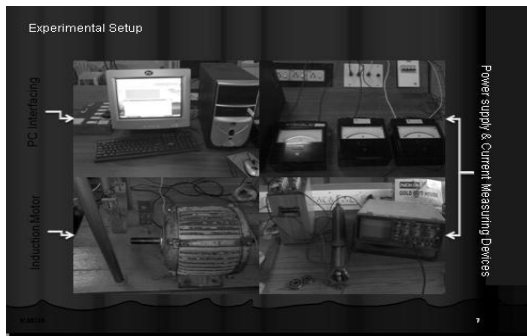
**Figure 2.3 Testing Equipment &
Experimental Setup**

Figure 2.4 Bearings Drilled With Holes

Experimentation has been conducted by using faulty bearings. Bearing fault is created by drilling holes of various diameter (say 2mm or 3mm) in the race- ways both inner and outer which is similar to bearing faults

Two bearings of 6204Z and one bearing of 6203Z type were damaged and taken for experimental. While these are not realistic bearing failures, the artificial bearing faults produce characteristic fault frequencies and the type of fault is determined by the current spectra.

2.4 Motor Current Signature Analysis (MCSA)

From the bearing data sheet, the outside diameter of a 6204Z bearing is 47mm and inside diameter is 20 mm. Assuming that the inner and the outer races have the same thickness gives the pitch diameter as equal to 34.15mm *(D = 34.15mm)*. The bearing has eight balls *(N = 8)* with approximate diameters of 7.85mm *(d = 7.85mm)*. Assuming a contact angle $\theta = 0\circ$ and motor

operation at a rated shaft speed of 960rpm, the characteristic race frequencies of the shaft-end bearing are calculated using equation 2.2 and 2.3 as *fo* = 73.93 Hz and *fi* = 118.07 Hz for the test motor.

The results show that for a bearing which was damaged from the outer raceway and inner races with holes, the characteristic frequencies could be seen in the current spectrum.

The current spectra of the test motor are shown in figures (figure 2.5 to figure 2.7). The frequency components in the current spectra of the motor with defective bearing at shaft end are $|fe + 1 \cdot fo| = 123.93$, $|fe + 2 \cdot fo| = 197.86$, $|fe+3 \cdot fo| = 271.79$ *and* $|fe+4 \cdot fo| = 345.72$ Hz frequencies. It is shown that these components are visible only in the plots of the defective bearing.

Current measurements for the damaged bearings were repeated under loaded operation of the induction machine. The current harmonics predicted for rated speed operation can still be found in the current spectrum. This indicates that, regardless of the load level of the machine, the bearing components are still detectable in the current spectrum. It is important to note that the frequency components produced by the bearing defect are relatively small when compared to the rest of the current spectrum. The largest components present in the current spectra occur at multiples of the supply frequency and are caused by saturation, winding distribution and supply voltage.

2.5 Experimental Results

The current spectrum of healthy and faulty machine is shown in Figures (Figure 2.5 to Figure 2.7).
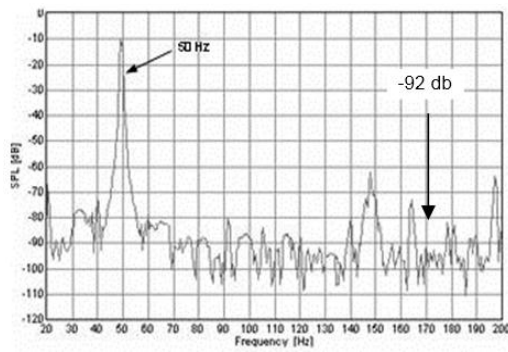
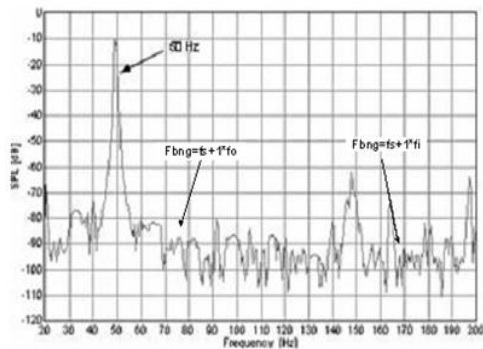**Figure 2.5 Current Spectrum for Healthy Machine**

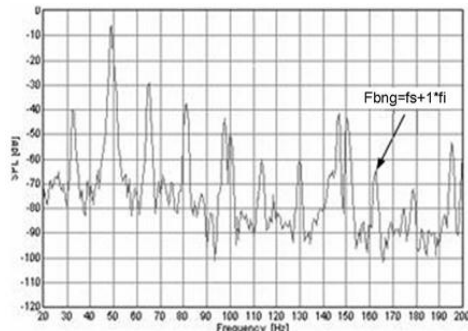**Figure 2.6 Current Spectrums for Faulty Machine with Shaft End**

Figure 2.7 Current Spectrums for Faulty Machine Fan End

A comparative study has been made with the current spectrum of motor with healthy bearing and with a faulty one in both shaft end and fan end of the test motor, which is shown in Figures (Figure 2.5 to Figure 2.7). Also the data at different characteristic frequencies are shown in the Table 2.2 & 2.3.

Table 2.2 Experimental Results of the Defective Shaft End Bearing

| Characteristic Frequencies	Outer Race f_o = 73.43			Inner Race f_i =118.067		
M (harmonic order)	1	2	3	1	2	3
Frequency (Hz) At f $_{(bng)}$	118.3	192.4	269.4	163.06	276.13	414.20
Harmonic amplitude for faulty machine in (dB)	-28.68	-27.45	-34.66	-36.19	-34.46	-35.68
Harmonic amplitude for healthy machine in (dB)	-37.25	-36.48	-47.83	-41.08	-43.40	-52.02

Table 2.3 Experimental Results of the Defective Fan End Bearing

Characteristic Frequencies	Outer Race f_o = 73.43			Inner Race f_i =118.067		
M (harmonic order)	1	2	3	1	2	3
Frequency (Hz) At f $_{(bng)}$	121.1	194.22	262.33	169.89	275.79	400.69
Harmonic amplitude for faulty machine in (dB)	-34.57	-28.04	-40.17	-38.39	-35.89	-44.85
Harmonic amplitude for healthy machine in (dB)	-37.79	-36.19	-44.85	-40.33	-43.42	-46.11

III. STRUCTURE OF BP NETWORK FOR FAULT DETECTION

An artificial neural network is composed of neurons with a deterministic activation function. The neural network is trained by adjusting the numerical value of the weights will contain the non-linearity of the desired mapping, so that difficulties in the

mathematical modeling can be avoided. The BP training algorithm is used to adjust the numerical values of the weights and the internal threshold of each neuron. The network is trained by, initially selecting small random weights and internal threshold and then presenting all training data. Weights and thresholds are adjusted after every training example is presented to the network; until the weight converges or the error is reduced to acceptable value. Figure 3.1 shows the structure of BP Network for Fault Detection [13], [14].
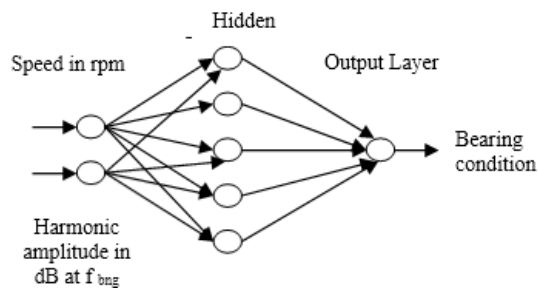
Figure 3.1 Structure of BP Network for Fault Detection

3.1 Simulation Results

Table 3.1 shows that input and output of the BP network.

Table 3.1 BP Network Input and Output

Speed (RPM)	Harmonic Amplitude (dB)	Target
860	-45	0
880	-65	0.5
920	-75	1
950	-85	1
Average error		1.57

Feed forward neural networks with two layers are used. The network consists of two input neuron, five hidden neurons and one output neuron. BP algorithm is used for training. The activation function in the first layer is log–sigmoid, and the output layer transfer function is tan-sigmoid function is the output layer. The training function used is trainlm. Figure 3.2 shows the performance characteristics of the BP network.
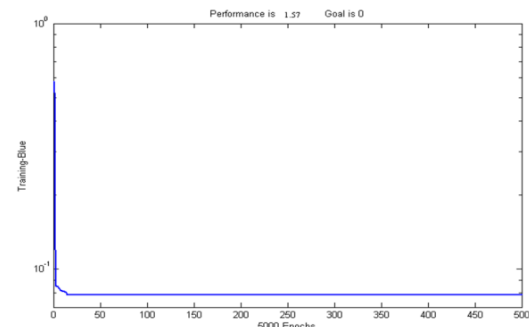
Figure 3.2 Epoch Vs Error Characteristics

IV. CONCLUSION

The bearing fault detection methods for three phase induction motor have been implemented using neural network. The technique is based on monitoring the current spectrum and speed .The current spectrum value and speed are taken as the inputs for neural fault detector .The performance of neural network fault detection is in terms of percentage of error. From the simulation results, it is inferred that the neural network diagnosis gives the reduced percentage error .Hence neural network based fault diagnosis is the effective method for fault detection. The fault detection scheme has been implemented in real time. The experimental results were presented.

REFERENCES

1) R.C.Kryter et al., "Condition monitoring of machinery using motor current signature analysis," sound Vib. pp 14-21, sept.1989.
2) A.J.M. Cardoso et al., "Computer-aided detection of air gap eccentricity in operating three-phase induction motors

by park's vector approach," IEEE Trans. Ind. Applicat. , Vol.29, pp.897-901, sept. / Oct. 1993.

3) R.R schoen et al., "Effects of time-varying loads on rotor fault detection in induction machine," IEEE Trans. Ind. applicat. Vol: 31, pp: 900-906, July/Aug., 1995.

4) R.r. Schoen et al., "Evaluation and implementation of a system to eliminate arbitrary load effects in current –current based monitoring of induction machines ,"IEEE Trans. Ind., Vol.33, pp.1571-1577, Nov./Dec. 1997.

5) J Penman et al., "Condition monitoring of electrical drives," Proc. inst. Elect. Eng., pt. b, Vol. 133, pp 142-148, May 1986.

6) S. Chen et al., "A new approach to motor condition monitoring in induction motor drives, "IEEE Trans. Ind. Applicat., Vol.30, pp. 905-911 July/Aug. 1994.

7) M.E Steele, R .A Ashen, and L.G.knight, "An electrical method for condition monitoring of motors," in int. conf. Ele. Mach. –Design and applicat. July 1982, no 213.pp, 231-235.

8) "Methods of motor current signature analysis," Elec. Mach. Power sys, vol: 20, no 5, pp 463-474, sept, 1992.

9) R.R. Schoen et al, "Motor bearing damage detection using stator current monitoring, "IEEE Trans. ind. applicat., vol 31, pp.1274-1279 Nov/Dec 1995.

10) Riddle J 1955 Ball bearing maintenance (Norman, OK: Univ. of Oklohama).

11) Eschmann P,Hasbargen L,weigand K, "1958" - Ball and roller bearings : Their theory, design, and application (London: K G Heyden)

12) R.L.Schiltz,"Forceing frequency identification of rolling element bearings," sound vib., Pp.16-19, May 1990.

13) Fiorenzo fillippetti, Giovanni Franceschini , and Peter vas, "Recent development of induction motor drives fault diagnosis using AI techniques ", IEEE Trans. Industrial Electronics.,vol.47,No.,pp.994-1003.

14) Fillippetti. F, Franceschini.G and Tassoni.C, "Neural networks aided on line Diagnosis of induction Motors Faults", IEEE Trans. Idl. Applicat., Vol: 31, No 4 , pp 316-323,1995

15) Rajasekaran .S and Vijayalaksmi Pai.G.A, "Neural networks, Fuzzy Logic and Genetic Algoritham Synthesis and Application's", Prentice Hall of India, 1995